RSC Advances

ROYAL SOCIETY OF CHEMISTRY

www.rsc.org/advances

Journal Name

ARTICLE

Inverse effects of supporting electrolytes on the electrocatalytic nitrate reduction activities in a Pt|Nafion|Pt-Cu type reactor assembly

Received 00th January 20xx,
Accepted 00th January 20xx

DOI: 10.1039/x0xx00000x

www.rsc.org/

Mohammad A. Hasnat [a,*], Jamil A. Safwan [a], M.A. Rashed [b], Zidnia Rahman [a], Mohammed M. Rahman [c], Yuki Nagao [b], Abdullah M. Asiri [c]

In this article, effects of Cl^- and SO_4^{2-} ions on the electrocatalytic nitrate reduction activities in a sandwich type reactor assembly have been illustrated. It has been noticed that a Pt|Nafion|Pt−Cu assembly offers it's best efficiency in the absence of any supporting electrolytes. The Pt−Cu thin layers adsorb chloride and sulphate ions firmly, and this adsorption blocks the H^+ reducing sites at the cathode end of the catalytic assembly leading to decrease of catalytic efficiency. In the presence of chloride and sulphate ions, reduction reactions of NO_3^- and NO_2^-, respectively, are relatively favoured.

Keywords: Electrocatalysis, Nitrate reduction, Supporting electrolytes, Impedance, Proton conductivity.

Introduction

Nitrate reduction process is exclusively important to the researchers from the view of environmental context.[1–25] On the other hand, numerous useful chemicals such as NH_3, N_2, NO, N_2O, NO_2, HNO_2, NH_2OH may be synthesized by reducing nitrate ions.[8–32] Therefore, studies of nitrate reduction reactions (NRR) are essential from the view of both environmental and synthetic issues. Catalytic hydrogenation of nitrate ions has been widely studied in the literature.[6-9] However, this process is cost effective and materials often cannot be reused. In this connection, development of suitable catalytic materials and their application in an electrolysis reactor is relatively inexpensive and easily operative. The geometry of a reactor plays crucial roles concerning reactivity, selectivity and reproducibility of a catalytic process.[17] In the case of conventional electrolysis reactor, the catalytic surfaces often become poisoned and/or loss stability.[27] To overcome this problem, sandwich type membrane reactor has been fabricated as shown in Fig. 1.[21,27] These types of reactors (M │membrane │M, M= Pt, Pd, Pt–Pd) have been successfully employed for the selective oxidation of various organic compounds.[33–37] In a conventional reactor, ample of supporting electrolyte is prerequisite as it can decrease the solution resistance. Although, conductivity requirement is successfully satisfied in such a case, but it requires an additional process to separate the synthesized products from the supporting electrolytes. However, such a constraint is not applicable for the M │membrane │M type reactors since a conductive membrane serves as an electrolytic junction between the anode and the cathode. In a previous article, we have reported that reproducible catalytic performance (of Pt-Cu cathode) can be observed if a pure nitrate containing solution is electrolysed,[17] but impacts of supporting electrolytes have never been investigated pertaining to reduction reactions using these types of reactors. In addition, in the coastal regions of many areas (e.g. Bangladesh), various electrolytes such as NaCl, Na_2SO_4 are coexisted along with $NaNO_3$.[38] Thus, if someone intends to reduce nitrate ions from saline water using this type of reactor, the electrocatalytic ability/responses of the electrode assembly must be checked in the presence of some common electrolytes such as NaCl, Na_2SO_4 etc. Hence, the aim of this article is to unveil the responses of these two very common electrolytes on the activities of the sandwich type membrane reactor. Since copper metal is known as one of the best electrocatalysts in attaining NRR, [15,17, 19] a Pt │Nafion │Pt−Cu reactor was fabricated to evaluate the NRR activities in the presence of NaCl and Na_2SO_4 electrolytes.

Experimental

In order to prepare a membrane–electrode assembly (MEA),

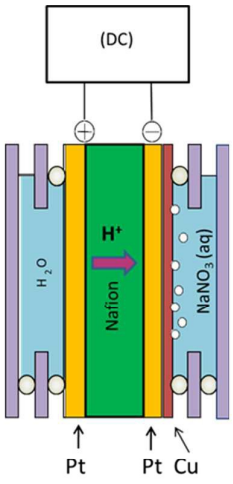

Fig. 1 Schematic diagram of electrolysis reactor.

platinum was first chemically deposited from H_2PtCl_6 on a Nafion−117 membrane (Wako Incorp. Japan) by using a reduction mixture of sodium borohydride and sodium hydroxide. At first, a slice of Nafion membrane (2 cm × 3 cm) was sand blasted and dried at 110 ^oC; then was merged into 200 ml of a 7.5 mM solution of H_2PtCl_6. Next, a mixed solution of 2.0 M $NaBH_4$ and 4.0 M NaOH was added to the membrane containing system at a rate of 2.0 ml/h. At the same time, the reaction mixture was heated from 35 ^oC at a rate of 5 ^oC/h upto 70^oC. The Pt plating on both sides of the Nafion membrane was completed within 12 hours. The total geometric area of the each surface was 6 cm^2, where the resistivity of the plated surfaces was less than 10 Ωcm^{-1}. The as prepared assemblies were first washed by dilute HCl, then were ultrasonic vibrated for 30s to remove adhered $NaBH_4$ and NaOH from the surface, and finally dried at 110 °C in air. The as prepared MEAs were then installed in a self-assembled rigid acrylate frame to fabricate the reactor as shown in Fig. 1, where the cathode surface separated from the anode surface by the H^+ conducting Nafion membrane. To perform electrolysis, the cathode and the anode chambers were filled with 8 ml aqueous solution of $NaNO_3$ and water, respectively, which was previously connected with a DC supplier. In order to analyze the concentration changes of NO_3^-, NO_2^- and NH_4^+ with time, a portion of 20 µl was collected from the solution in the cathode compartment at a constant interval and diluted to 5 ml. The concentration changes of NO_3^-, NO_2^- and NH_4^+ were measured by an ICA–2000 model (DKK–TOA Corporation) ion chromatograph. In order to estimate catalytic performance, the rate constant (k) was evaluated on the assumption that the concentration of NO_3^- (C) decreases following first order kinetics, i.e., $C = C_0 \exp(-k_1 t)$, where C_0 is the initial concentration and t is time (min).The electrochemical investigations were carried out under thermostatic and N_2−atmosphere condition using an Autolab PGSTAT128N instrument (Metrohm Autolab B.V.). All potentials in the present work have been reported with respect to Ag|AgCl (sat. KCl) reference electrode. In order to prepare Pt−Cu catalytic surface, a Pt disk (ϕ = 2 mm) was placed in a 0.01 M $CuSO_4$ solution then the potential was cycled six times between 0 and 1.0 V at a scan rate of 100 mVs^{-1}. This yielded the electrodeposition of Cu overlayers on the Pt disk. Prior to employing for NRR experiments, the as−prepared electrode was washed thoroughly with water and the potential was swept repeatedly between 0 and 1.5 V in a 0.05 M KCl solution until stable cyclic voltammograms were obtained. In order to record CVs, the system was kept at a rest potential of −0.1V for 30s, then the potential scanning of nitrate containing solution was performed between 0 and −1.4V at various scan rates. Similar electrochemical setup was also used for EIS studies. The surface morphology was analysed by Energy dispersive X–ray analysis (EDS) coupled with FESEM, JEOL, Japan). The FTIR spectra of Nafion membrane were recorded on potassium bromide (KBr) pellets with an SHIMADZU IR spectrometer (Model No-dxp 400). At first, a Nafion membrane sheet was sand blasted, washed several times with distilled water, dried and chipped into three pieces. The dried one piece of Nafion membrane was penetrated into 0.1 M NaCl solution, where another piece in 0.1 M Na_2SO_4 solution for 60 min. The soaked Nafion membrane was washed with distilled water and dried in an oven at 40 ˚C. To record FTIR spectra, the dried Nafion membrane was chipped as small as possible and then grinded it with KBr to form pellets. The X–ray photoelectron spectra (XPS) study was performed using Kratos Axis−Ultra DLD spectrometer, using Al Kα radiation source (1486.6 eV). Energy calibration and component separation were carried out by the bundled software using pure Gaussian profiles with a linear background.

Results and discussion

Electrolysis

In order to investigate the responses of chloride and sulphate ions on the activity of sandwich type membrane reactor (Pt|Nafion|Pt−Cu; shown in Fig. 1), pertaining to NRR, 180 min long electrolysis experiments were performed.

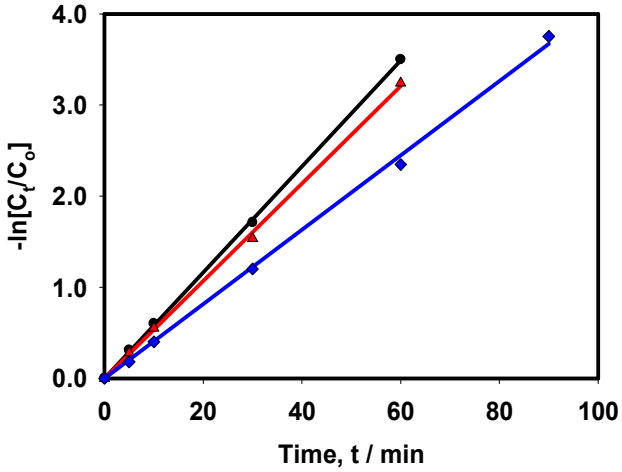

Fig. 2. Linear fittings of first order kinetic equation with respect to 0.05 M $NaNO_3$ reduction reaction in the presence of (●) water only, (▲) 0.01M NaCl and (■) 0.01M Na_2SO_4. [DC input 100 mA, catholyte 8 ml, 300K].

Figure 2 shows that electrolysis data were well−matched with respect to first order rate equation ($r^2 \geq 0.99$), whereas **Table 1** summarizes the corresponding analytical data. In the absence of any supporting electrolytes, nitrate ions reduced with a rate constant (k_1) of 42.8 $\times 10^{-3}$ min^{-1}. However, in the presence of 0.01 M NaCl and 0.01 M Na_2SO_4 electrolytes, k_1 decreased to 40.6×10^{-3} min^{-1} and 35.3×10^{-3} min^{-1}, respectively. This observation suggests that the catalytic assembly exhibited it's highest efficiency while a pure nitrate containing solution was electrolyzed alone. The presence of chloride or sulphate ions adversely affected the performance of the catalytic surface, and between these two spectator anions; sulphate ions were inferior to chloride ions. In the sandwich type reactor, water molecules are oxidized on the anode surface producing molecular oxygen and protons. Under the applied potential, protons are migrated towards the cathode surface through the conducting Nafion membrane. These protons are next reduced at the cathode surface to form adsorbed hydrogen atoms and/or molecules as per following mechanism.[24]

Anode (Pt):

$$H_2O_{ads} \rightarrow 2H^+ + \frac{1}{2}O_2 + 2e^- \quad (1)$$

$$H^+(\text{anode}) \rightarrow H^+(\text{cathode}) \text{ (migration)} \quad (2)$$

Cathode (Pt–Cu):

$2H^+ + 2e^- \rightarrow 2H_{ads} \rightarrow H_{2,\,ads}$ (3)

Table 1 Effects of supporting electrolytes on 0.05 $NaNO_3$ reduction

Parameter	AE	NaCl	Na_2SO_4
k_1/ 10^{-3} min^{-1}	42.8	40.6	35.3
NO_3^- removal_/%	100	100	100
S (NO_2^-) /%	45.0	21.0	11.6
S (NH_4^+) /%	4.2	7.0	8.5

100mA, 295K, 180 min, Cathode: 18 atom %Cu +82atom%Pt), 0.01M NaCl/ Na_2SO_4, AE: absence of supporting electrolytes

The adsorbed hydrogen atoms participate in the catalytic hydrogenation reactions (shown in scheme 1) to reduce nitrate ions.[8] Because of circuit requirement reasons and catalytic ability of adsorbed hydrogen atoms, H^+ conductivity of Nafion (reaction 2)

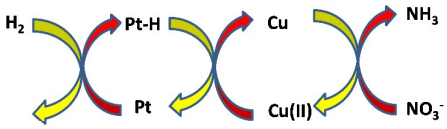

Scheme 1. Catalytic hydrogenation reactions of nitrate ions on the Pt–Cu surface.

determines the catalytic performance of the reactor. Thus, in order to elucidate the catalytic dissimilarities, in the presence of chloride and sulphate ions, the electrochemical and spectroscopic studies have been performed as stated bellow.

EIS studies

Electrochemical impedance spectroscopy (EIS) is a powerful tool to elucidate the efficiency of various diffusionless processes like binding of the electroactive species, electron transfer reactions at the surface, H^+ conductivity through a medium and different interfacial processes (e.g analyte adsorption, oxide formation etc).[39-42] Since NRR also occurs due to heterogeneous electron transfer reactions, the comparative binding of the catalyst (Pt−Cu) with specific reactant (NO_3^-) in the presence of supporting electrolytes has been studied using a three−electrode system. The EIS spectra have been classically presented in the form of a complex plane plot, where Z′ is the real and Z″ is the imaginary part of impedance as shown in Fig. 3, which was obtained in the presence of 0.1M supporting electrolytes (NaCl and Na_2SO_4). For an ideal non polarizable system, the circuit comprises a series connection of solution resistance (R_s) with a parallel combination of a charge transfer resistance (R_{ct}) and a double layer capacitance (C_d). The impedance of such a system may be written as -[41]

$$Z(\omega) = Z_{R_s}(\omega) + Z_{pl}(\omega) \quad (4)$$

Where, $Z_{R_s}(\omega)$ and $Z_{pl}(\omega)$ represent the impedance of solution resistance (R_s), and parallel combination of double layer capacitance (C_d) and transfer resistance (R_{ct}).The equation (4) is often rewritten in terms of reactance as [42]

$$Z(\omega) = [\, Z_{R_s}(\omega) + \frac{R_{ct}}{1+\omega^2 R_{ct}^2 C_{dl}^2}] + j[\frac{-\omega R_{ct}^2 C_{dl}}{1+\omega^2 R_{ct}^2 C_{dl}^2}] \quad (5)$$

Here, the first and second parentheses represent the real and the

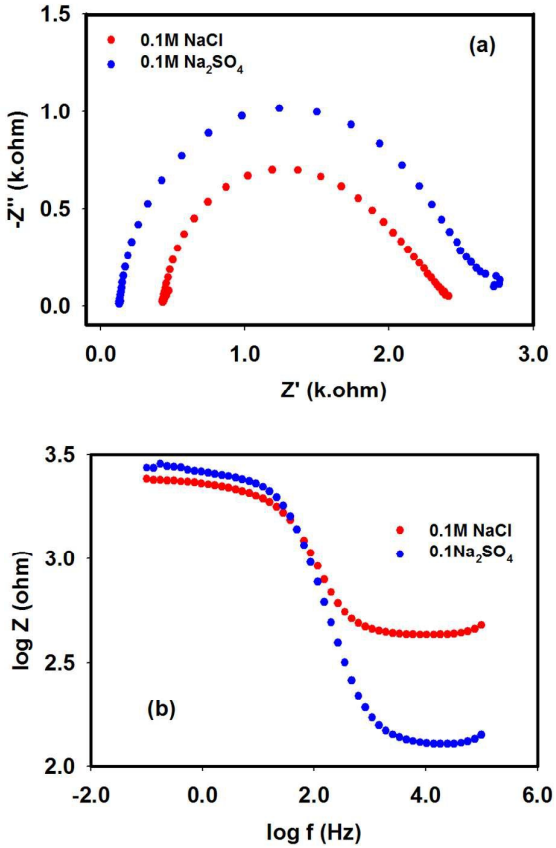

Fig. 3. EIS spectra recorded with Pt–Cu electrode in the presence of NaCl and Na_2SO_4 supporting electrolytes (0.1M in each case) at -1.2 V. (a) Complex plan plot and (b) Bode plot.

imaginary parts, respectively, of the impedance. As can be seen from the complex plan plots (see Fig. 3a) both in the chloride and sulphate media, the impedance of the system exhibited semicircles at −1.2 V, which is typical for a kinetic controlled process. At 100 kHz, the capacitive impedance was short−circuited, which practically diminished the R_{ct}. As a consequence, only R_s remained at the high frequency intercept.

Table 2 EIS properties of Pt−Cu surface -in presence of chloride and sulphate ions measured at −1.2 V

Medium	R_s/ohm	R_{ct} / ohm	C_{dl} / μFcm^{-2}
0.1 M NaCl	427	1990	25.57
0.1 M Na_2SO_4	125	2601	19.11

Meanwhile, the low frequency intercept represent the sum of R_s and R_{ct}. Therefore, the diameter of the semicircle represents R_{ct}.[40] It can be noticed from equation (5) and Fig. 3a that the maximum of the Z'' occurred at $Z' = R_s + R_{ct}/2$, which denotes the specific frequency of the

charge transfer process (ω_{max}). It can be seen from Figure 3b that the Bode magnitude of the system provided two breakpoints; starting from the high frequency edge, the first breakpoint corresponds to the time constant τ_1:

$$\tau_1 = \frac{1}{\omega_1} = \frac{R_s R_{ct} C_{dl}}{R_s + R_{ct}} \quad (6)$$

and, the second breakpoint represents time constant τ_2;[42]

$$\tau_2 = \frac{1}{\omega_{max}} = R_{ct}\, C_{dl} \quad (7)$$

It is to note that as the chloride and sulphate ions are non−reducible species at the working potential, therefore, the diameter of the complex plane plots (hence R_{ct}) should measure the resistance due to dissolution of Cu(II) and/or Cu(I) species on the Pt−Cu surface. Considering these facts, different EIS properties have been tabulated in Table 2. According to the tabulated data, it is clear that Pt−Cu surface was more resistive and less capacitive in the sulphate medium compared to a chloride medium.

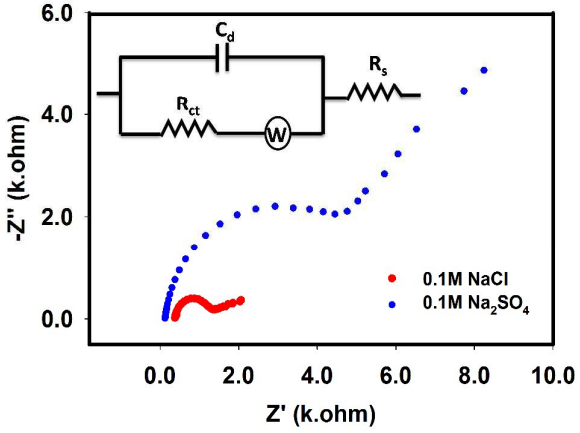

Fig. 4. EIS spectra recorded with Pt–Cu electrode for 0.015 M $NaNO_3$ in the presence of 0.1 M NaCl and 0.1 M Na_2SO_4 at – 1.0 V. Inset shows equivalent circuit.

By taking the advantages of these EIS information, next impedance spectra of 0.015 M $NaNO_3$ were recorded in the presence of supporting 0.1M electrolytes as shown in Fig. 4. At the working potential of −1.0V, the complex plan plots provided arcs (with the diameter associated to the charge transfer resistance, R_{ct}, originated due to reduction of the NO_3^- ions at the interface of the electrode) followed by a diagonal straight . Thus, in this case, kinetic control process coupled with the mass transfer process, where the simplified Randle's circuit was modified by introducing Warburg impedance (*W*) as shown in the inset of Fig. 4 to model the mixed control process. As expected, the larger semi-circular diameter (hence larger R_{ct} value) is seen in presence of sulphate ions in comparison with that of chloride ions. This observation suggests that the increased surface coverage of sulphate ions on the Pt−Cu surface, due to either specific or nonspecific adsorption, exposed less number of sites for the nitrate reduction reactions. Consequently, the evaluation of R_{ct}, and C_{dl} schemes that in comparison with chloride ions, sulphate ions impeded Pt−Cu surface more prominently in executing reduction of nitrate ions.

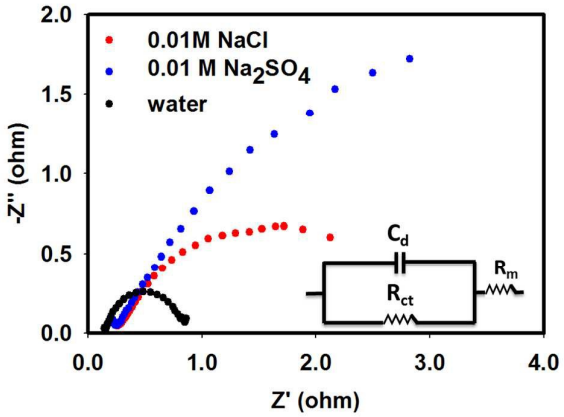

Fig. 5. EIS spectra of Pt|Nafion|Pt-Cu system recorded in the presence and in the absence of 0.01 M supporting electrolytes (NaCl and Na_2SO_4) at working potential of −0.8V . Inset shows associated equivalent circuit.

However, in the reactor (Fig. 1), the conducting membrane (solid electrolyte) acts as an electrolytic junction between the anode and cathode where the protons are the charge carriers. In order to illustrate the functions of supporting electrolytes on H^+ conducting parameters (hence reactivity) of the Pt|Nafion|Pt−Cu assembly, EIS spectra were finally recorded in the presence and absence of supporting electrolytes by installing this catalytic assembly in the reactor shown in Fig. 1. The cell impedance was measured at various frequencies ranging from 100 kHz to 0.001 Hz applying an AC excitation voltage of −0.8 V. For this particular membrane assembly, the electrical equivalent circuit (shown in the inset of Fig. 5)

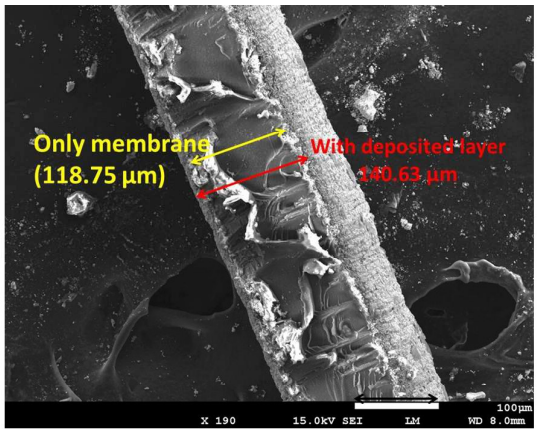

Fig.6. SEM image of the cross-section of Pt|Nafion|Pt assembly.

represents electron transfer, charging of the double layer and migration of H^+ through the membrane. The real component of the EIS spectra at 100 kHz was credited almost exclusively to the

resistance of the membrane (R_m), which may be used to calculate proton conductivity of the membrane. The active area of the membrane was 3 cm^2 and it's thickness was 118.75 µm (determined from the SEM image of the cross−section of Nafion membrane, Fig. 6). Using these data, the specific H^+ conductivity (C_{H^+}), due to reaction (2), through the membrane in the presence of pure water was evaluated as 0.027 Scm^{-1}. However, when water was replaced with 0.01 M NaCl and 0.01 M Na_2SO_4 solution, in the separate experiments, C_{H^+} was decreased to 0.016 Scm^{-1} and 0.015 Scm^{-1}, respectively. This means that H^+ conductivity of Nafion membrane was greatly interrupted in the presence of supporting electrolytes. It is to note that the semi-circular arc, which appeared in the frequency range 10 to 10 kHz, was attributed to the charging of the electrode−solution interface (C_{dl}). The charge transfer resistance (R_{ct}) was associated to reduction of H^+ (given by reaction 3) at the edge of lower frequency region. It is clear from Fig. 5 that the shapes of the semi-circular arcs, hence C_{dl} and R_{ct} were highly penetrated by the supporting electrolytes. The least R_{ct} was noticed when no supporting electrolyte was present in the system, and it increased following an order of *pure water* < *NaCl* < Na_2SO_4. This observation is consistent with the performance of the electrolysis data reported in Table 1, i.e, NRR rate was inhibited in the membrane reactor in the presence of chloride and sulphate ions following a reverse trend of R_{ct} increase.

Voltammetry

Figure 7 shows CVs of nitrate (Fig.7a) and nitrite (Fig.7b) reduction reactions with corresponding voltammetric responses of supporting electrolytes (Fig. 7c) recorded with an Pt-Cu electrode. Nitrate ions are reduced on a catalytic surface using a consecutive reaction trail ($NO_3^- \rightarrow NO_2^- \rightarrow NH_3$), where nitrite ions are evolved as intermediates. It can be seen from Table 1 that electrolysis of a pure nitrate solution yielded highest nitrite selectivity (45%), which decreased to 21% and 11.6% in the presence of chloride and sulphate ions, respectively. This observation suggests that supporting electrolytes can promote reduction of intermediate nitrite ions, where SO_4^{2-} ions had stronger influences over the Cl^- ions in minimizing the concentration of intermediate nitrite ions. To elucidate this phenomenon, voltammetric experiments were performed. Figure 7a shows the CVs of 0.015 M $NaNO_3$ solution recorded using a Pt−Cu electrode at a scan rate of 50 mVs^{-1} in the presence of 0.1 M NaCl and 0.1 M Na_2SO_4 electrolytes. In the double layer region, the waves E1 and E2 are associated to the reduction of Cu(I) and Cu(II) species, respectively. Meanwhile, the E5 and E6 correspond the oxidation of Cu(0) to Cu(II) and Cu(I), respectively. From the CVs, it is clearly seen that oxidation−reduction currents (hence total charge) of copper species were more intense in the presence of sulphate ions than in the presence of chloride ions. Such difference suggests that under the sulphate environment, more Cu(II)/Cu(I) species were generated than in the chloride environment, which is consistent with the EIS studies. However, in the kinetic region, the E3 and E4 waves denote the reduction of nitrate and nitrite ions, respectively, as per following reactions. [24]

at (E3): $NO_3^-{}_{ads} + H_2O_{ads} + 2e^- \rightarrow NO_2^-{}_{ads} + 2OH^-{}_{ads}$ (8)

at (E4): $NO_2^-{}_{ads} + 5H_2O_{ads} + 6e^- \rightarrow NH_{3ads} + 7OH^-{}_{ads}$ (9)

The E3 wave generated more current in the presence of chloride ions than in the presence of sulphate ions implying that reaction (8) was relatively favoured in the chloride medium. But opposite effect is seen in the case of E4 wave, i.e, nitrite reduction current (reaction 9) in the sulphate medium suppressed that generated in the chloride medium. As a consequence, least nitrite selectivity was noticed

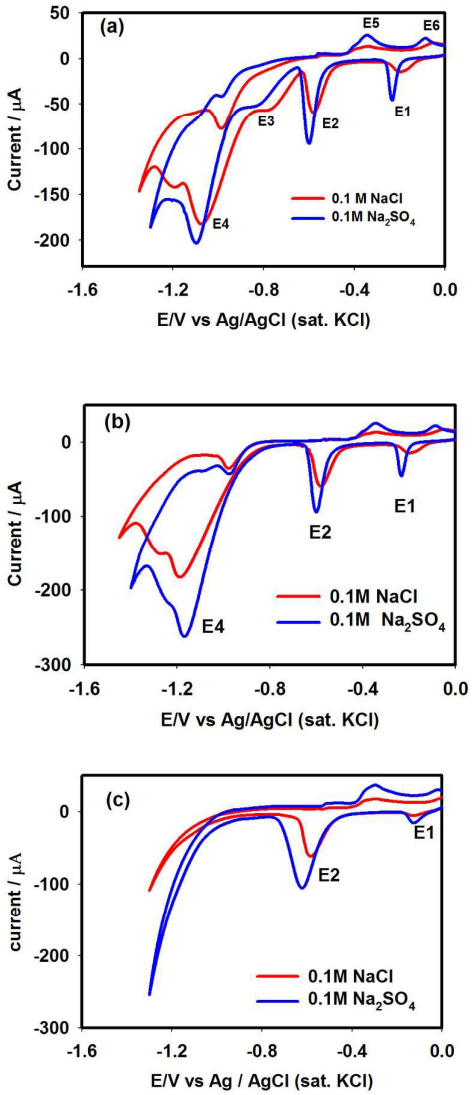

Fig.7. Cyclic voltammograms of 0.015 M $NaNO_3$ (a) and 0.015 M $NaNO_2$ (b) recorded with the Pt–Cu electrode at a scan rate of 50 mVs^{-1} using NaCl and Na_2SO_4 supporting electrolytes. Figure (c) represents CVs of supporting electrolytes (NaCl and Na_2SO_4).

during the electrolysis experiments in the sulphate medium as reported in Table 1. In order to justify these results, CVs of NO_2^- ions were next recorded in the presence of chloride and sulphate ions as shown in Fig.7b. It is let alone to mention that the CV profiles of nitrite ions notably matched with those observed for the reduction of nitrate ions.

Surface morphology

In this present study, catalytic surface contained 18 atom% Cu and 82 atom% Pt, which was confirmed by the energy dispersive X−ray analysis (Fig. 8a). The SEM image of the Pt−Cu surface shows that the catalytic particles existed as an aggregated network having 61−132 nm in size (Fig. 8b).

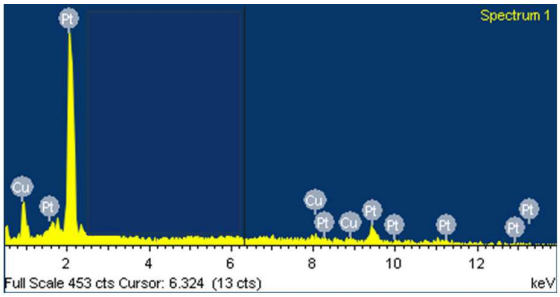

(a)

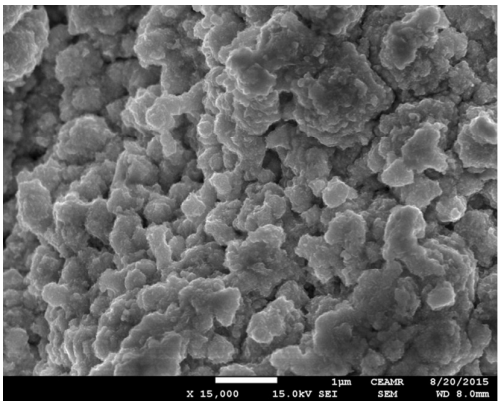

(b)

Fig. 8. Surface morphology of Pt−Cu surface; (a) EDS spectra and (b) SEM image.

FTIR study

In order to assess the reasons of decreased H^+ conductivity and increased charge transfer resistance (R_{ct}) in the presence of supporting electrolytes at the cathode surface of the reactor shown in Fig. 1, FTIR analysis of Nafion membrane was performed. Figure 9 shows the FTIR spectra of Nafion membrane recorded before and after soaking it in 0.1 M sulphate and chloride solutions. Since the Nafion membrane is proton conducting by nature, it was assumed that cation (Na^+) might be entrapped by the Nafion membrane, which might induce nonspecific adsorption of counter anions. The IR spectrum of the Nafion membrane shows the characteristic vibrations of Nafion at 1220 cm^{-1} (asymmetric C−F stretching). The peaks at 1156 cm^{-1} are assumed for symmetric C−F stretching. The peaks at 1057 cm^{-1} are attributed for S−O stretching. The C−F stretching of ($-CF_2-CF(R)-CF_2-$) groups shows the vibrations at 982 cm^{-1}. The other characteristic peaks of Nafion were found at 970 cm^{-1} (C−O−C stretching), 653 cm^{-1} (asymmetric O−S−O bending), 636 cm^{-1} (C−S stretching), 554 cm^{-1} (asymmetric C−F bending), and 512 cm^{-1} (symmetric O−S−O bending) according to a previous report.[43] However, none of these bands was penetrated by

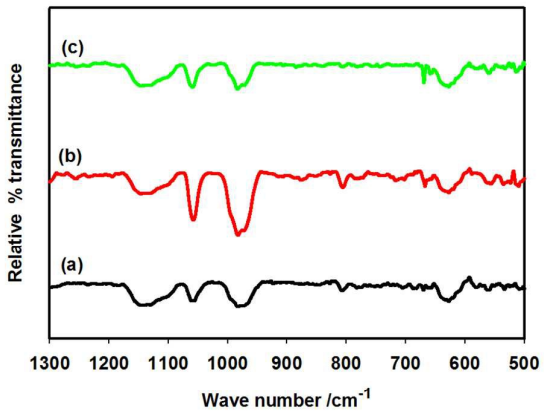

Fig. 9. FITIR spectra of pure Nafion (a), 0.1M NaCl soaked Nafion (b), and 0.1 M Na_2SO_4 soaked Nafion (c).

the chloride or sulphate ions. This observation suggests that nonspecific adsorption of chloride or sulphate ions by the Nafion membrane did not play any role in deciding reactor's performance. It was rather assumed that sulphate and chloride ions were adsorbed by the Pt−Cu layers deposited on the Nafion membrane, which probably blocked the H^+ reducing sites, and decreased the reactor's performance accordingly.

XPS study

The adsorption characteristics of chloride and sulphate ions on the Pt−Cu surface were investigated with X−ray photoelectron spectroscopy (XPS) analysis. The Cu $2p_{3/2}$ core energy level was employed to study the oxidation state of Cu surface. The linear background subtraction and Gaussian peak fitting of the broad Cu $2p_{3/2}$ XPS spectra represents a major peak at ~ 932.2 eV and relatively a small peak at 934.8 eV (see Fig. 10(a and b)). The major peak has been attributed for Cu(0) and/or Cu(I).

Table 3 The XPS data of Cu $2p_{3/2}$ peak in presence of NaCl and Na_2SO_4

Binding energy of Cu $2p_{3/2}$ (eV)			FWHM of Cu $2p_{3/2}$ (eV)		% Cu (II)
Medium	Cu (0) /Cu(I)	Cu (II)	Cu (0) / Cu (I)	Cu (II)	
SO_4^{2-}	932.1	934.8	1.5	2.8	11.25
Cl^-	932.2	934.8	1.5	2.8	9.62

% Cu(II) was obtained from deconvolution of Cu $2p_{3/2}$ peaks.

However, Cu(0)/Cu(I) could not be determined directly by the deconvolution because of very similar binding energies. [44] These peaks can be distinguished by LMM−2 auger transition in XPS spectra, which are 568 eV and 570 eV for Cu(0) and Cu(I) respectively.[45] In this specimen, we observed this peak at 567 eV in both of chloride and sulphate ion adsorption cases. From this fact,

we considered that this major peak is attributed due to Cu(0). However, this peak is in slightly higher binding energy in comparison with pure metallic copper (932.6 eV).[46] This discrepancy may arise due to the interaction of Cu with Pt (Figure not shown). Peak at 934.8 eV with board FWHM value (2.8 eV) has been attributed to the existence of Cu(II). The broaden peak shape of Cu (II) as compared to the major one (Cu(0)/Cu(I)) is due to coupling between unpaired electron (d^9) (multiple splitting) in the paramagnetic cupric ions.[47, 48] Moreover, the shake−up satellite structure centered at a binding energy of 943 eV, also denote the presence of Cu(II) species. This satellite peak can only be ascribed to the charge transfer transition to unfilled d−orbital of Cu atom. In the case of Cu(0)/Cu(I), there is a filled (d^{10}) ground state configuration. In this case, no charge transfer is possible and no satellite peak can be observed.[48, 49] Binding energy, FWHM and Cu(II)/Cu(0) ratio obtained from the deconvolution of Cu $2p_{3/2}$ peak is presented in Table 3.Figure 10 (c and d) shows the XPS fine scan spectra of S 2p and Cl 2p. From the tabulated results, it is seen that 11.25% of Cu(II) was formed on the sulphate treated Pt−Cu surface,

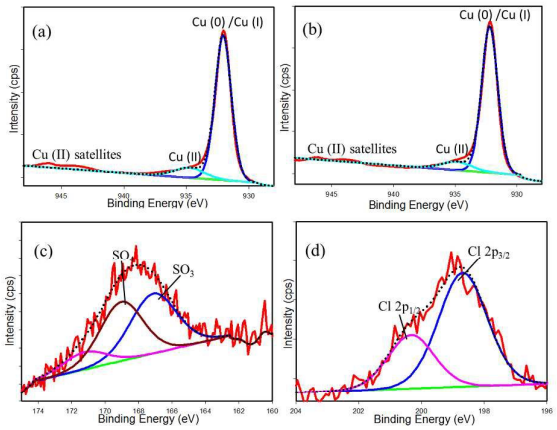

Fig. 10. (Top) XPS fine scan spectra Cu $2p_{3/2}$ of Cu modified Pt sample (a) Cu surface dipped in sulphate solution (b) Cu surface dipped in chloride solution (c) S 2p (d) Cl 2p.

and this quantity was decreased to 9.62% while the surface was treated in the chloride medium. This may happen due to strong interactions of SO_4^{2-} ions with Cu species of Pt−Cu electrode rather than chloride ions under identical reaction condition. This observation is consistent with CV and EIS results. In Figure 10(c), two intense S 2p features are seen to be appeared at 167.1 eV and 169.0 eV indicating the attribution of SO_3 and SO_4 species, respectively.[50] Rest small peak at higher binding energy (171.2 eV) may be attributed to charging of sulphur. In the case of deconvolution of Cl 2p, the two peaks at 198.7 eV and 200.3 eV represent the binding energies of Cl $2p_{3/2}$ and Cl $2p_{1/2}$, respectively. Thus, it is clear that the Pt−Cu layers adsorbed chloride and sulphate ions firmly, and this adsorption blocked the H^+ reducing sites at the cathode end of the catalytic assembly shown in Fig. 1. This study also confirms that formation of Cu(II) from Cu(0) was favoured by the adsorption of sulphate ions more prominently than the adsorption of chloride ions. The existence of more Cu(0) species favoured the NO_3^- reduction, but the existence of slightly increased amount of Cu(II) and/or Cu(I) favoured reduction of NO_2^- ions.

Surface stability

Finally, stability of the Pt−Cu surface in the presence of electrolytes was evaluated by measuring corrosion rate. Figure 11 shows the polarization curves of the Pt−Cu surface in the form of Tafel plots. The corrosion potential (E_{corr}) in the presence of chloride ions was −0.09 V. Meanwhile, this value shifted to −0.03 V in the presence of sulphate ions. From the slopes of V−shaped curves, the corrosion rate of Cu species was determined to be 5.5×10^{-4} and 14.0×10^{-4}

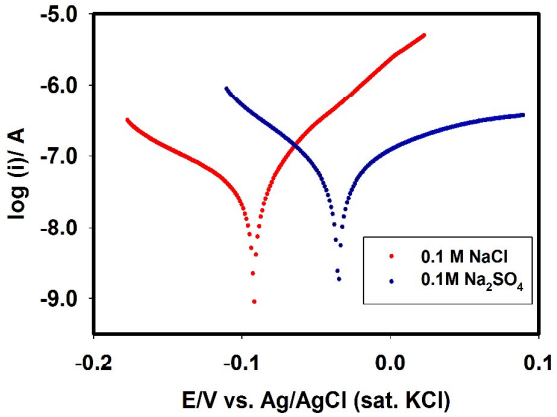

Fig. 11. Polarization curves of Pt−Cu surface in the presence of NaCl and Na_2SO_4.

mm/year in the presence of chloride and sulphate ions, respectively. This observation suggests that chloride ions were less aggressive than sulphate ions to destabilize the surface. This was because chloride ions generated less Cu(I)/Cu(II) species than those generated by the sulphate ions.

Summary

A sandwich type reactor assembly (Pt | Nafion | Pt−Cu) can show best reduction efficiency when no supporting electrolytes are present in the reactor. The anions (chloride and sulphate ions) have no interactions with electrolytic junction (Nafion membrane), rather they are adsorbed on the Pt−Cu surface. In comparison, presence of sulphate ions attributed more charge transfer resistance, generated more Cu(II) species, induced more corrosion of catalytic particles and attained less NRR rate than those were exhibited in the presence of chloride ions. Since Cl^- and SO_4^{2-} ions can deactivate the catalytic performance, the reactor may not be suitable (in the presence of these anions) for operation from the view of reproducible performance. However, in terms of long term use, the concentration of these anions might be minimized, possibly by separating them using other techniques (such as precipitation etc). Conversely, a noble point that a sulphate adsorbed Pt−Cu surface could reduce nitrite ions more efficiently than a chloride adsorbed surface.

Acknowledgement

The authors acknowledge Prof. Masato Machida, Department of Nano Science and Technology, Kumamoto University, Japan for providing required materials. The World Academy of Sciences (TWAS) is acknowledged greatly for finanicial support (Ref:14−050 RG/CHE/AS_G; UNESCO FR 34028605) to Mohammad A. Hasnat. Shahjalal University of Science and Technology research center is acknowledged for a partial financial supports.

Notes and References

[a] *Department of Chemistry, School of Physical Sciences, Shahjalal University of Science and Technology, Sylhet–3100, Bangladesh*
[b] *School of Materials Science, Japan Advanced Institute of Science and Technology, 1−1 Asahidai, Nomi, Ishikawa 923−1292, Japan*
[c] *Center of Excellence for Advanced Material Research (CEAMR) and Chemistry department, Faculty of Science, King Abdulaziz University, Jeddah 21589, P.O. Box 80203, Saudi Arabia*

**Corresponding author (M.A. Hasnat)*
Department of Chemistry, Shahjalal University of Science and Technology, Sylhet–3114, Bangladesh
Email: mahtazim@yahoo.com, mah–che@sust.edu
Phone/Fax (b): 88–0821–715752

1 N. F. Gray. *Drinking Water Quality: Problems and Solutions*, *Wiley and Sons Ltd., Chichester*, 1994, 21.
2 A. Pintar, J. Batista and J. Levec, *Chem. Eng. Sci.,* 2001, **56**, 1551.
3 A. E. Tugtas and S. G. Pavlostathis, *Biotechnol. Bioeng.,* 2007, **97**, 1448.
4 A. Pintar, J. Batista and J. Levec, *Water Sci. Tech.,* 1998, **37**, 177.
5 S. Horod, K. D. Vorlop, T. Tacke and M. Sell, *Catalysis Today,* 1993, **17**, 21.
6 F. Epron, F. Gauthard, C. Pineda, J. Barbier, *J. Catal*. 2001, **198**,309.
7 F. Gauthard,F. Epron, J. Barbier, *J. Catal*..2003, **220**, 182.
8 N. Barrabés, J. Just, A. Dafinov, F. Medina, J. L. G. Fierro, J. E. Sueiras, P. Salagre and Y. Cesteros, *Appl. Catal. B,* 2006, **62**, 77.
9 S. Kerkeni, E. Lamy-Pitara, J. Barbier, *Catal.Today*, 2002, **75**, 35.
10 W. Siriwatcharapiboon, Y. Kwon, J. Yang, R. L. Chantry, Z. Li, S. L. Horswell and M. T. M. Koper, *ChemElectroChem.,* 2014, **1**, 172.
11 M. Duca, M. O. Cucarella, P. Rodriguez and M. T. M. Koper, *J. Am. Chem. Soc*., 2010, **132**, 18042.
12 M. A. Hasnat, N. Ahamad, S. M. Nizam Uddin and N. Mohamed, *Appl. Surf. Sci.,* 2012, **258**, 3309.
13 J. F. van der Plas and E. Barendrecht, *Electrochim. Acta,* 1979, **25,** 1463.
14 M. S. Alam, M. A. Hasnat, M. A. Rashed, M. R. Miah and I. S. M. Saiful, *Electrochim. Acta,* 2012, **76**, 102.
15 G. E. Dima, A. C. A. de Vooys and M. T. M. Koper, *J. Electroanal. Chem.,* 2003, **15**, 554.
16 Y. Wang, Y. Sakamoto and Y. Kamiya, *Appl. Catal. A,* 2009, **361**, 123.
17 M. A. Hasnat, M. A. Islam and M. A. Rashed, *RSC Adv.,* 2015, **5**, 9912.
18 H. Cheng, K. Schot and P. A. Chiristensen, *J. App. Echem.,* 2005, **35**, 551.
19 D. Reyter, G. Chamoulaud, D. Belanger and L. Roue, *J. Elect. Anal. Chem.* 2006, **596**, 13.
20 I. Katsounaros, D. Ipsakis, C. Polatides and G. Kyriacou, *Electrochim. Acta,* 2006, **52**, 1329.
21 M. A. Hasnat, M. A. Islam, S. M. Borhanuddin, M. R. U. Chowdhury and M. Machida, *J. Molecular. Catal. A: Chemical,* 2010, **317**, 61.
22 M. A. Hasnat, M. S. Alam, M. H. M.–ul. Karim, M. A. Rashed and M. Machida, *Appl. Catal. B: Environ.,* 2011, **107**, 294.
23 M. A. Hasnat, M. A. Rashed, S. Ben Aoun, S. M. Nizam Uddin, M. Saiful Alam, S. Amertharaj, R. K. Majumder and N. Mohamed, *J.Molecular Catal. A,* 2014, **243**, 383.
24 M. A. Hasnat, S. Ben Aoun, S. M. Nizam Uddin, M. Mahbubul Alam, P. P. Koay, S. Amertharaj, M. A. Rashed, M. M. Rahman and N. Mohamed, *Appl. Catal. A,* 2014, **478**, 259.
25 M. A. Hasnat, I. Ishibashi, K. Sato, R. Agui, T. Yamaguchi, K. IKeue and M. Machida, *Bull. Chem. Soc. Jpn.,* 2008, **12**, 1.
26 M. Machida, K. Sato, I. Ishibashi, M. A. Hasnat and K. Ikeue, *Chem. Commun*., 2006, **7**, 732.
27 M. A. Hasnat, M. R. Karim and M. Machida, *Catal. Commun*., 2009, **10**, 1975.
28 M. da Chunha, J. P. I. De Souza and F. C. Nart, *Langmuir.,* 2000, **16**, 771.
29 S. Amertharaj, M. A. Hasnat and N. Mohamed, *Electrochim. Acta,* 2014, **136**, 557.
30 D. Reyter, D. Belanger and L. Roue, *Electrochim. Acta,* 2008, **53**, 5977.
31 A. Anastasopoulos, L. Hannah and B. E. Hayden, *J. Catal.,* 2013, **305**, 27.
32 Y. Y. Birdja, J. Yang and M. T. M. Koper, *Electrochim. Acta,* 2014, **140**, 518.
33 Z. Ogumi, S. Ohashi and Z. Takehara, *Electrochim. Acta,* 1985, **30**,121.
34 Z. Ogumi, H. Yamashita, K. Nishio, Z. I. Takehara and S. Yoshizawa, *Electrochim. Acta,* 1983, **28**, 1687.
35 K. Otuska and I. Yamanaka, *Appl. Catal.,* 1986, **26**, 401.
36 G. R. Dieckmann and S. H. Langer, *J. Appl. Electrochem.* 1997, **27**, 1.
37 G. R Dieckmann and S. H Langer, *Electrochim. Acta,* 1998, **44**, 437.
38 R. K. Majumder, M. A. Hasnat, S. Hossain, Keita Ikeue and Masato Machida, *J. Hazard. Mater.,* 2008, **159**, 536.
39 J. R. Macdonald, *Impedance spectroscopy, Annals*. *Biomedi. Eng.*, 1992, **20**, 289.
40 A. Bogomolova, E. Komarova, K. Reber, T. Gerasimov, O. Yavuz, S. Bhatt and M. Aldissi, *Anal. Chem.,* 2009, **81**, 3944.
41 L. R. F. Allen and J. Bard, *Electrochemical Methods: Fundamentals and Applications, Wiley, 2nd edition*, 2000.
42 B. A. Lasia, "Electrochemical impedance spectroscopy and it's applications," in Modern Aspects of Electrochemistry, B. E. Conway, J. O. M. Bockris and R.White, Eds., *Springer, New York, NY, USA,* 2002, 143–248.
43 M. Laporta, M. Pegoraro and L. Zanderighi, *Phys. Chem. Chem. Phys.,* 1999, **1**, 4619.
44 T. Ghodselahi, M. A. Vesaghi, A. Shafiekhani, A. Baghizadeh and M. Lameii, *Appl. Surf. Sci.,* 2008, **255**, 2730.
45 J. Y. Park, J. Y. S. Jung and W. K. Cho, *Appl. Surf. Sci.,* 2006, **252**, 2877.
46 V. Hayez, A. Franquet, A. Hubin and H. Terryn, *Surf. Interface Anal.*, 2004, **36**, 876.
47 A. Rosencwaig and G. K. Wertheim, *J. Electron Spectrosc. Relat. Phenom.*, 1972/1973, **1**, 493.
48 K. S. Kim, *J. Electron Spectrosc. Relat. Phenom.,* 1974, **3**, 217.
49 J. Ghijsen, L. H. Tjeng, J. van Elp, H. Exkes, J. Westerink, G. A. Sawatzky and M. T. Czyzyk, *Phys. Rev. B* 1988, **38**, 11322.
50 J. A. Rodriguez, T. Jirsak, A. Freitag, J. C. Hanson, J. Z. Larese and S. Chaturvedi, *Catal. Lett.* 1999, **62**, 113.

Inverse effects of supporting electrolytes on the electrocatalytic nitrate reduction activities in a Pt|Nafion|Pt-Cu type reactor assembly

Mohammad A. Hasnat, Jamil A. Safwan, M.A. Rashed, Zidnia Rahman, Mohammed M. Rahman , Yuki Nagao, Abdullah M. Asiri

A Pt|Nafion|Pt-Cu assembly can exhibit it's best reduction reaction efficiency in absence of any supporting electrolytes. Adsorption of supporting electrolytes decreases efficiency by registering increase of charge transfer resistance.